Muon-spin-rotation and magnetization study of metal-organic magnets based on the dicyanamide anion

2001 J. Phys.: Condens. Matter 13 2263

(http://iopscience.iop.org/0953-8984/13/10/318)

INSTITUTE OF PHYSICS PUBLISHING JOURNAL OF PHYSICS: CONDENSED MATTER

J. Phys.: Condens. Matter **13** (2001) 2263–2270 www.iop.org/Journals/cm PII: S0953-8984(01)17964-6

Muon-spin-rotation and magnetization study of metal–organic magnets based on the dicyanamide anion

Th Jestädt[1], M Kurmoo[2], S J Blundell[1], F L Pratt[3], C J Kepert[4,6], K Prassides[5], B W Lovett[1], I M Marshall[1], A Husmann[1], K H Chow[1,7], R M Valladares[1,8], C M Brown[5] and A Lappas[5]

[1] Oxford University Department of Physics, Clarendon Laboratory, Parks Road, Oxford OX1 3PU, UK
[2] IPCMS, 23 rue du Loess, BP 20/CR, 67037 Strasbourg Cédex, France
[3] RIKEN-RAL, ISIS, Rutherford Appleton Laboratory, Didcot OX11 0QX, UK
[4] Inorganic Chemistry Laboratory, Oxford University, South Parks Road, Oxford OX1 3QR, UK
[5] School of Chemistry, Physics and Environmental Science, University of Sussex, Falmer, Brighton BN1 9QJ, UK

Received 12 October 2000, in final form 7 February 2001

Abstract

We report the results of a study of the metal–organic magnets $M^{II}[N(CN)_2]_2$, where M^{II} = Ni, Co and Mn, using bulk magnetization and muon-spin relaxation (μSR). Implanted muons are sensitive to the onset of long-range magnetic order in each of these materials and strong muon-spin relaxation is observed in the paramagnetic state due to low-frequency fluctuations of the electronic moments in the 10^9–10^{10} Hz range. The size of the muon-spin relaxation in the paramagnetic state can be related to the magnitude of the transition-metal-ion moment. Very strongly damped oscillations are observed below the magnetic transition temperature in $Co[N(CN)_2]_2$.

1. Introduction

In recent years there has been a growing effort aimed at achieving an understanding of molecule-based magnets and obtaining novel molecular magnetic materials with high transition temperatures [1]. There is also a strong drive towards developing engineering materials with combined optoelectronic and magneto-optical properties. The dicyanamide ion, $[N{\equiv}C{-}N{-}C{\equiv}N]^-$, has been found to be a promising choice as a ligand in assembling novel metal–organic ferromagnets and ferrimagnets (see references [2–7]) because it aligns divalent transition metal ions in such a way that their magnetic orbitals are approximately orthogonal. It is a small ligand and so can give rise to well defined structures with large orbital overlaps. It

[6] Present address: School of Chemistry, Building F11, University of Sydney, NSW 2006, Australia.
[7] Present address: Department of Physics, Lehigh University, 16 Memorial Drive East, Bethlehem, PA 18015, USA.
[8] Present address: Departamento de Física, Facultad de Ciencias, UNAM, Apartado Postal 70-542, Mexico DF, 04510, Mexico.

0953-8984/01/102263+08$30.00

contains delocalized π-electrons which enhance indirect exchange (principally superexchange) between metal sites. In this paper we concentrate on the pure metal complexes, $M^{II}[N(CN)_2]_2$, containing M^{II} = Ni (d^8, $S = 1$), M^{II} = Co (d^7, $S = 3/2$) or M^{II} = Mn (d^5, $S = 5/2$). X-ray diffraction [3] and neutron scattering experiments [8] suggest that these compounds are isostructural, and that they adopt an orthorhombic form of the rutile structure [2, 3] similar to those of $CrCl_2$ and CuF_2. For the Ni and Co materials, the ground state is ferromagnetic. Below the ferromagnetic transition temperature the spins are ordered collinearly [8] with magnetic moments of 2.61 μ_B ($Co[N(CN)_2]_2$) and 2.21 μ_B ($Ni[N(CN)_2]_2$) oriented along the c-axis. The magnetic structure of $Mn[N(CN)_2]_2$ consists of two sublattices which are antiferromagnetically coupled and canted. The spin orientation is mainly along the a-axis with a small component along the b-axis [9].

Implanted muons have been extensively used to study organic and molecular magnets (for reviews see [10, 11]). In this paper we present the results of muon-spin-rotation (μSR) studies of these materials which provide information concerning the internal field and the spin dynamics in the paramagnetic state.

2. Experimental details

The samples were prepared as described in reference [3], where details of the characterization may be found. Magnetization measurements were performed using a SQUID magnetometer. μSR experiments were carried out both at the ISIS facility of the Rutherford Appleton Laboratory (UK) and at the Paul Scherrer Institute (Switzerland). In a μSR experiment [12–14] spin-polarized positive muons are stopped in a target sample. The muons (lifetime 2.2 μs) usually occupy interstitial positions in the crystal. In the dicyanamide magnets the muons appear to form diamagnetic states and we do not believe that a muon is likely to pick up an electron during the stopping process. The observed quantity is the time evolution of the muon-spin polarization. Each muon decays into two neutrinos and a positron, the latter particle being emitted preferentially along the instantaneous direction of the muon spin. Recording the time dependence of the positron emission directions therefore gives direct information about the spin polarization of the ensemble of muons. The behaviour of the polarization depends on the local magnetic field at the muon site. In our experiments, positrons are detected by detectors placed forward (F) and backward (B) of the initial muon polarization direction. Histograms $N_F(t)$ and $N_B(t)$ record the number of positrons detected in the two detectors as a function of time following the muon implantation. The quantity of interest in a μSR experiment is the positron asymmetry function, defined as

$$A(t) = \frac{N_F(t) - \alpha N_B(t)}{N_F(t) + \alpha N_B(t)} \tag{1}$$

where α is an experimental calibration constant. In our experiments, samples of a typical mass of 3 g were packed in a silver foil (thickness 25 μm) envelope (typical dimensions are 20 mm $\times$ 17 mm $\times$ 2 mm) and mounted on a silver backing plate in the cryostat. Silver is used because it gives a non-relaxing muon signal and hence only contributes an additive constant to $A(t)$. The Earth's magnetic field was compensated to better than 10 μT. For a detailed review of the μSR technique and its application to magnetic materials, see reference [15].

3. Results and discussion

The Curie temperature, T_C, of the ferromagnetic samples was determined for each sample from the small-field magnetization, the peak in the real part of the a.c. susceptibility and a non-zero

value of the imaginary part of the a.c. susceptibility. We find $T_C = 21.2(2)$ K for $Ni[N(CN)_2]_2$ and $T_C = 9.7(2)$ K for $Co[N(CN)_2]_2$. The magnetization data were fitted to a mean-field model, with good agreement over the whole temperature range (see figures 1(b) and 1(d)), although there are small deviations in the middle part of the ordered-state temperature range: the mean-field model overestimates the magnetization for Ni and slightly underestimates it for Co. These deviations are very small and are not visible in figures 1(b) and 1(d). The Weiss constants are 22.7(2) K for $Ni[N(CN)_2]_2$ and 9.7(6) for $Co[N(CN)_2]_2$. The magnetization data were also fitted to a power law in the vicinity of T_C to give the critical exponent β. In agreement with the mean-field fit we find that β is very close to 0.5 (for $Ni[N(CN)_2]_2$, $\beta = 0.52(3)$; for $Co[N(CN)_2]_2$, $\beta = 0.47(4)$). The measured magnetic susceptibility of $Mn[N(CN)_2]_2$ (not shown) fits to the Curie–Weiss law between 17 and 300 K with a Weiss constant of $-25.0(1)$ K. There is a transition to long-range order in this material at 16.0 K, below which it is a canted antiferromagnet [3, 9]. The fitted β in this case is 0.37(1) [3]. The canting angle is too small to be observed by means of neutron scattering, but is estimated to be 0.05° [16].

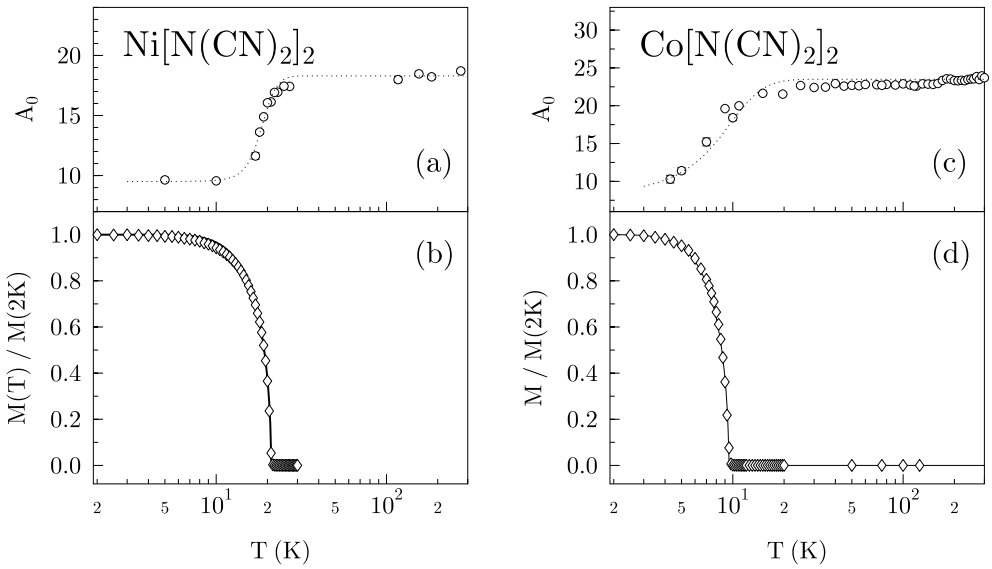

Figure 1. Magnetization and μSR data for ((a), (b)) $Ni[N(CN)_2]_2$ and ((c), (d)) $Co[N(CN)_2]_2$. The upper panels show the initial asymmetry of the positron decay obtained from the μSR. The dashed lines are a guide to the eye. The lower panels show the normalized magnetization in an applied field of less than 0.01 mT (estimated). The solid line through the magnetization data shows the best fit assuming a mean-field model.

Typical μSR spectra from measurements at the ISIS pulsed muon facility for the three compounds are displayed in figure 2. An indicator of a phase transition to a magnetically ordered state is either the development of oscillations in the μSR asymmetry function $A(t)$ below T_C or, in cases where the oscillations are too fast to be resolved experimentally, a loss of initial asymmetry, $A_0 = A(0)$, which sets in below T_C. This loss is observed here (see figure 2) and displayed in detail in figures 1(a) and 1(c) for $Ni[N(CN)_2]_2$ and $Co[N(CN)_2]_2$. The loss of initial asymmetry correlates well with the magnetic transition observed in our magnetization measurements and represents a reduction of approximately $\frac{2}{3}$ of the signal due to the sample in each case.

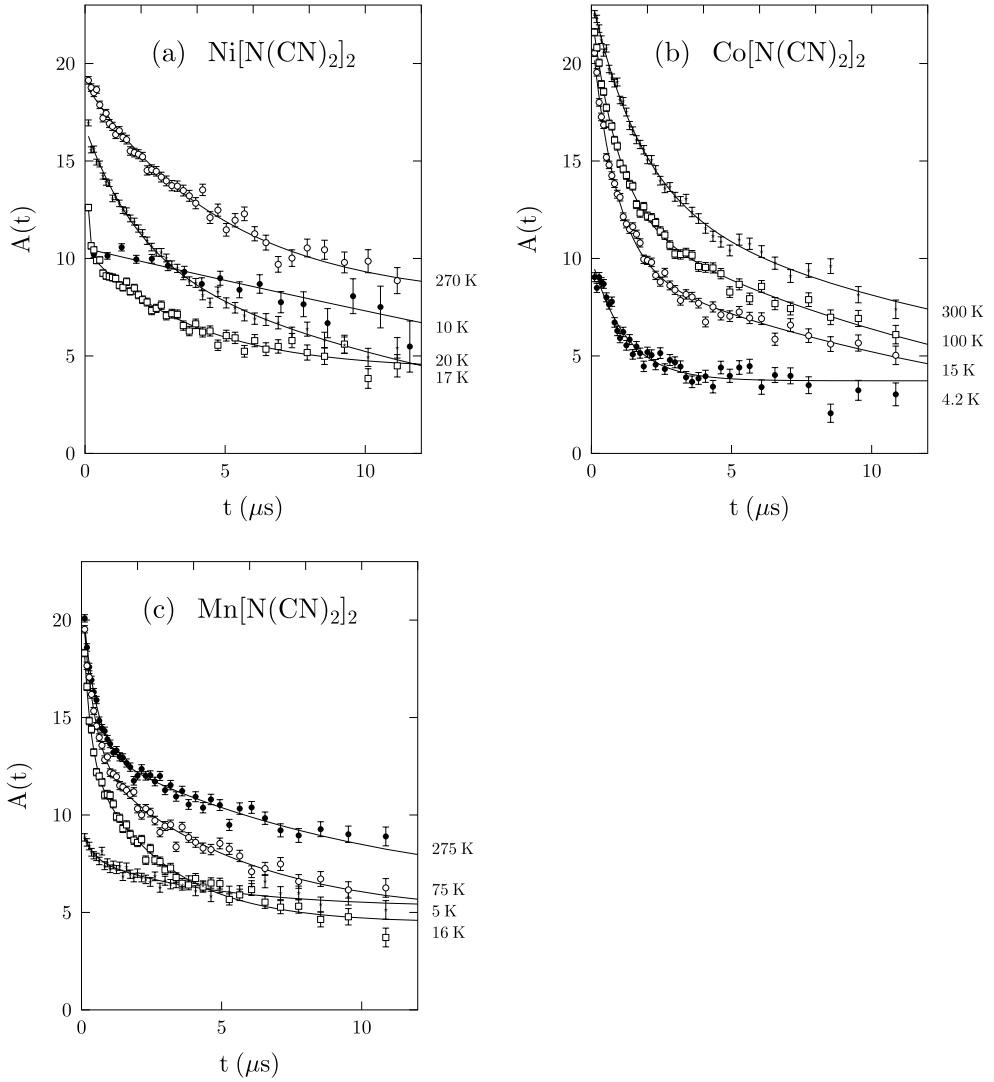

Figure 2. μSR data for (a) $Ni[N(CN)_2]_2$, (b) $Co[N(CN)_2]_2$ and (c) $Mn[N(CN)_2]_2$.

We note that at temperatures well above the transition temperature there is still substantial relaxation of the muon polarization. This indicates that the spins responsible for the relaxation of the muon spins are fluctuating at a rate which is in the muon time window. To confirm that the relaxation is dynamic in origin, we applied a longitudinal magnetic field B_L to each compound at several different temperatures and observed that the relaxation was not quenched by the field. As an example, data for $Co[N(CN)_2]_2$ at 60 K demonstrating this are shown in figure 3. The longitudinal-field data also demonstrate that the relaxation is not due to some muoniated radical state which would quench much more rapidly in a magnetic field than we observe here. The zero-field data in the paramagnetic state for each compound were fitted to the functional form

$$A(t) = A_\perp e^{-(\lambda_\perp t)^\gamma} + A_\parallel e^{-\lambda_\parallel t} + A_{bg} \tag{2}$$

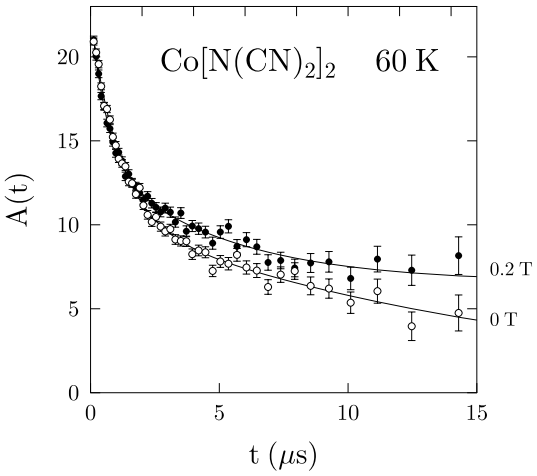

Figure 3. μSR data for $Co[N(CN)_2]_2$ at 60 K in zero field and in an applied longitudinal magnetic field of 0.2 T.

where $A_\perp$, $A_\parallel$ and A_{bg} are the oscillatory, relaxing and background amplitudes, $\lambda_\perp$ and $\lambda_\parallel$ are relaxation parameters and γ is a lineshape parameter. We have kept $A_\perp/A_\parallel = 2$ fixed. $\lambda_\parallel$ is typically much less than 0.1 MHz and is only weakly temperature dependent. The temperature dependence of $\lambda_\perp$ and γ for $Co[N(CN)_2]_2$ (the compound for which we have the most detailed data set) are shown in figure 4. We held $\gamma = 1$ fixed (corresponding to relaxation with a single time constant) over most of the temperature range but had to let it fall towards $\gamma \sim \frac{1}{2}$ as T_C was approached from above, demonstrating that fluctuations, with a range of time constants and/or amplitudes, set in as the critical region is entered. The parameter $\lambda_\perp$ is only weakly

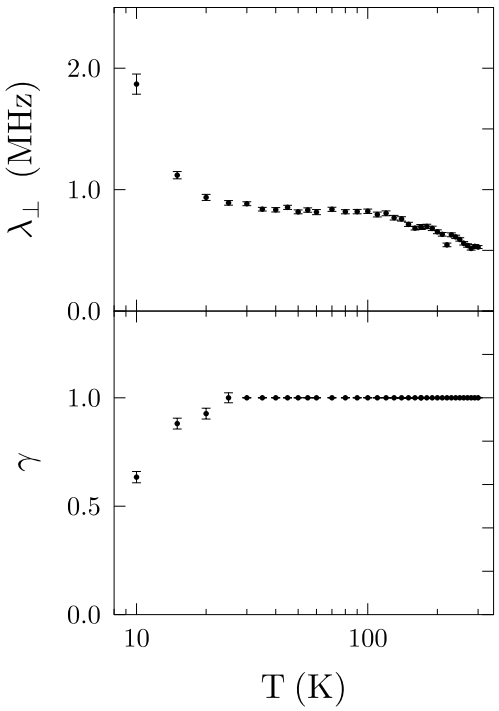

Figure 4. Temperature dependences of the relaxation rate $\lambda_\perp$ and lineshape parameter γ for $Co[N(CN)_2]_2$.

temperature dependent but begins to rise rapidly as T_C is approached.

It is possible to relate the relaxation rate to the fluctuation rate of the electronic moments using $\lambda = 2\Delta^2\tau$ [17] which is valid in a regime where $\tau^{-1} \gg \Delta$ and where a single time constant characterizes the relaxation. Here Δ/γ_μ is the width of the local magnetic field distribution, τ^{-1} is the fluctuation rate and $\gamma_\mu = 2\pi \times 1.355 \times 10^8$ s^{-1} T^{-1} is the gyromagnetic ratio of the muon. We assume Δ/γ_μ to be of the order of the magnetic field at the muon site at low temperatures (see below for $Co[N(CN)_2]_2$). It is apparent from figure 3 that the high-temperature relaxation becomes progressively larger as one moves from $Ni[N(CN)_2]_2$ to $Co[N(CN)_2]_2$ to $Mn[N(CN)_2]_2$. This is mainly due to the progressive increase in Δ which scales as the magnetic moment (2.21 μ_B for $Ni[N(CN)_2]_2$, 2.67 μ_B for $Co[N(CN)_2]_2$, 4.61 μ_B for $Mn[N(CN)_2]_2$ [8, 9]). The measured relaxation rates thus imply relatively slow electronic moment fluctuation rates τ^{-1} in the range 1–10 GHz which are responsible for producing the observed relaxation. This fluctuation rate is still much faster than $\gamma_\mu B_L$, explaining why the relaxation rate in a longitudinal field B_L (given by $\sim 2\Delta^2\tau/(1 + [\gamma_\mu B_L \tau]^2)$ [17]) is hardly affected. As shown below, the internal field below the transition temperature is $\sim$0.05 T in $Co[N(CN)_2]_2$. With fields of this magnitude, only fluctuations in the range 10^6 s$^{-1} \lesssim \tau^{-1} \lesssim 10^{11}$ s^{-1} produce observable depolarization within the timescale of μSR measurements. The fluctuations slow down as T_C is approached from above, and a quasistatic (on the muon timescale) local field is observed in the ordered state (see below).

In order to further investigate the ordered state we have carried out additional experiments on $Co[N(CN)_2]_2$ at the Paul Scherrer Institute. This facility has a higher time resolution and hence we were able to resolve (albeit highly damped) low-temperature oscillations in the

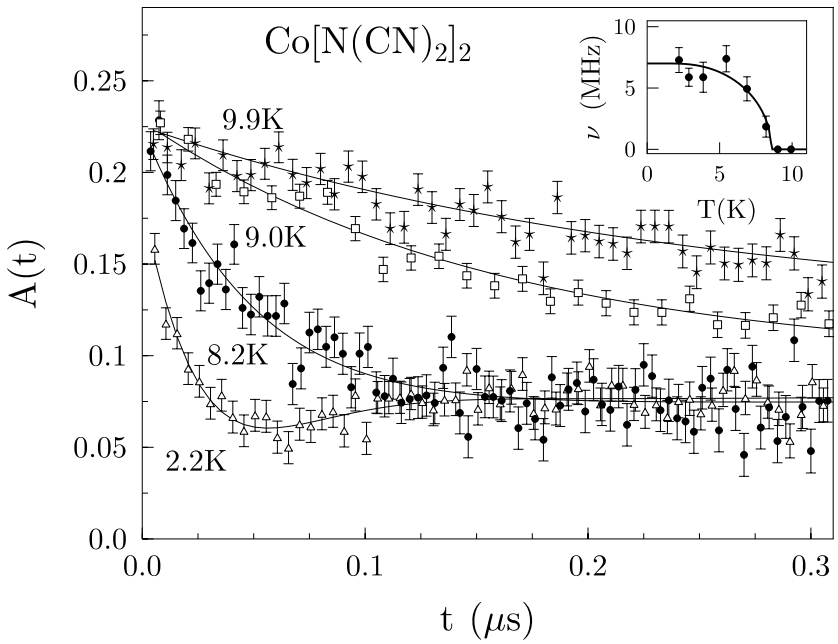

Figure 5. The temperature dependence of $A(t)$ for $Co[N(CN)_2]_2$ in a high-time-resolution experiment. The inset shows the temperature dependence of the fitted muon precession frequency which is proportional to the internal field at the muon site.

spectra; see figure 5. We have fitted these spectra for $T < T_C$ with the expression

$$A(t) = A_\perp e^{-\lambda_\perp t} \cos(2\pi\nu t + \varphi) + A_\parallel e^{-\lambda_\parallel t} + A_{bg} \quad (3)$$

where φ is a phase factor, $\nu = \gamma_\mu B/2\pi$ is the Larmor precession frequency and B is the magnetic field at the muon site. For the fits in the ordered temperature region we have also kept $A_\perp/A_\parallel = 2$ fixed. This is because in a polycrystalline sample, $\frac{2}{3}$ of the signal is due to regions in which the local field is perpendicular to the initial muon-spin polarization, and $\frac{1}{3}$ of the signal is due to regions in which the local field is parallel to the initial muon-spin polarization. The fits were performed over the restricted time range from 0 μs to 0.5 μs. We find that the temperature dependences of the relaxation $\lambda_\perp$ and the oscillation frequency ν are similar, and that the inhomogeneous linewidth $\lambda_\perp/2\pi\nu$ is approximately constant in the magnetically ordered regime. This might indicate that the large damping of the oscillatory signal is due to static depolarization and has its origin in the presence of various muon sites. Because of the very strong damping, functional forms other than equation (3) could fit the data. Nevertheless, it is clear from the minimum in the lowest-temperature data shown in figure 5 that a quasistatic field does develop at the muon site in the ordered state. The average magnetic field at the muon site as $T \to 0$ is found to be $\sim$0.05 T. As stated above, we can rule out a muoniated radical state because of the longitudinal-field data, but a number of diamagnetic muon sites in the crystal structure could be possible. However, some *dynamic* relaxation is also present, since the non-oscillatory component is also relaxing, as shown in the 4.2 K trace of figure 2(b). (This non-oscillatory component, which in the absence of dynamics often yields a '$\frac{1}{3}$ tail', can be very sensitive to dynamical effects [17].) The damping rates are much larger than those that are found in purely organic magnets [10], due presumably to the presence of these dynamical effects.

In conclusion, we have reported the results of a study of the metal–organic magnets $M^{II}[N(CN)_2]_2$, where M^{II} = Ni, Co and Mn, using bulk magnetization and μSR. We observe large muon-spin relaxation in the paramagnetic state which can be ascribed to low-frequency fluctuations of the electronic moments in the 10^9–10^{10} Hz range. Very strongly damped oscillations are observed below the magnetic transition temperature in $Co[N(CN)_2]_2$.

Acknowledgments

We acknowledge the support of CNRS (France) and the EPSRC (UK). We would like to thank the staff of the ISIS and PSI muon facilities for their assistance and Bill Hayes for numerous discussions about molecular magnets.

References

[1] Kahn O (ed) 1996 *Magnetism: a Supramolecular Function (NATO ASI vol C484)* (Dordrecht: Kluwer)
[2] Batten S R, Jensen P, Moubaraki B, Murray K S and Robson R 1998 *J. Chem. Soc., Chem. Commun.* 439
[3] Kurmoo M and Kepert C J 1998 *New J. Chem.* **22** 1515
[4] Kurmoo M and Kepert C J 1999 *Mol. Cryst. Liq. Cryst.* **334** 693
[5] Batten S R, Jensen P, Kepert C J, Kurmoo M, Moubaraki B, Murray K S and Price D J 1999 *J. Chem. Soc. Dalton Trans.* 2987
[6] Kurmoo M 1999 *Chem. Mater.* **11** 3370
[7] Manson J L, Kmety C R, Huang Q, Lynn J W, Bendele G M, Pagola S, Stephens P W, Liable-Sands L M, Rheingold A L, Epstein A J and Miller J S 1998 *Chem. Mater.* **10** 2552
[8] Kmety C R, Manson J L, Huang Q, Lynn J W, Erwin R W, Miller J S and Epstein A J 1999 *Phys. Rev.* B **60** 60
[9] Kmety C R, Huang Q, Lynn J W, Erwin R W, Manson J L, McCall S, Crow J E, Stevenson K L, Miller J S and Epstein A J 2000 *Phys. Rev.* B **62** 5576
[10] Blundell S J 1999 *Phil. Trans. R. Soc.* A **357** 2923

[11] Gatteschi D, Carretta P and Lascialfari A 2000 *Physica* B **289** 94
[12] Cox S F J 1987 *J. Phys. C: Solid State Phys.* **20** 3187
[13] Blundell S J 1999 *Contemp. Phys.* **40** 175
[14] Dalmas de Réotier P and Yaouanc A 1997 *J. Phys. C: Solid State Phys.* **9** 9113
[15] Schenck A and Gygax F N 1995 *Handbook of Magnetic Materials* vol 9, ed K H J Buschow (Amsterdam: Elsevier) pp 57–302
[16] Lappas A, Prassides K and Kurmoo M 2001 unpublished results
[17] Uemura Y J, Yamazaki T, Harshman D R, Senba M and Ansaldo E J 1985 *Phys. Rev.* B **31** 546